Geometrical and dynamical properties of homoclinic tangles in a simple Hamiltonian system

G. Contopoulos
Department of Astronomy, University of Florida, Gainesville, Florida 32611
and Department of Astronomy, University of Athens, GR 157 83-Athens, Greece

C. Polymilis
Department of Astronomy, University of Athens, GR 157 83-Athens, Greece
(Received 4 February 1992; revised manuscript received 26 May 1992)

We study, qualitatively and quantitatively, the forms of the asymptotic curves from an unstable periodic orbit in a simple Hamiltonian for various values of the energy. The asymptotic curves define two resonance areas and form infinite elongated "lobes." We give the exact (not schematic) forms of such lobes over long times, and formulate certain rules followed by them. The lengths of the lobes of order n are of the order of λ^n, where λ is the largest eigenvalue of the periodic orbit. The lobes surround the resonance areas, spiraling outwards, before going into the large stochastic region outside the resonances. This explains the "stickiness" property of the resonance areas over long times. As the energy increases, the number of rotations of the lobes decreases and the onset of chaos is faster. The lengths and the areas of the lobes increase considerably. The number of intersections of the lobes increases, and we find how new tangencies between the various lobes are formed. If the energy goes beyond the escape energy, certain lobes terminate at "limiting asymptotic curves" corresponding to asymptotic curves of the Lyapunov orbits at the various escape channels.

PACS number(s): 05.45.+b, 03.20.+i

I. INTRODUCTION

It is well known that the structure of the asymptotic curves from unstable periodic orbits on a surface of section is extremely complicated. Poincaré [1] wrote that "one will be impressed by the complexity of this figure, that I do not even try to draw." Many people made sketches of such curves, but often such sketches miss some important characteristics of the asymptotic curves. Examples of such cases will be given below. A qualitative discussion of the intersections of the "lobes," or "tongues," formed by the asymptotic curves was made by Guggenheimer and Holmes [2], Wiggins [3,4], Rom-Kedar and Wiggins [5], and Contopoulos [6]. These lobes form the so-called "homoclinic tangle" [2,4] that is considered to be a characteristic of chaos.

However we will show that the homoclinic tangle has some degree of order, at least for long times. Namely, the lobes formed by the asymptotic curves of a certain resonance do not fill immediately the total available stochastic region but they first make a number of rotations around the islands of stability corresponding to this resonance before visiting the whole stochastic region. The number of rotations depends on the energy of the system.

We have studied these phenomena in a simple Hamiltonian system. We give the lobes exactly (not schematically) for long times and derive certain qualitative and quantitative conclusions about their forms and the chaos that they generate in the homoclinic tangle.

For small energies the lobes make several rotations around the main islands of stability before extending to larger distances. As the energy increases the lobes become longer and deviate faster from the stability regions.

As the length of the lobes increases, we have new tangencies and new intersections of the various lobes that we study in some detail. These tangencies introduce new sets of stable orbits; therefore, chaos is not complete.

When the energy goes beyond the escape energy some particles escape to infinity. The problem then arises of what is the form of the lobes that lead to escapes. We find that the lobes form infinite spiral rotations around particular closed limiting asymptotic curves.

The phenomena that we describe in the present paper are both geometrical and dynamical. In fact the time dependence of the evolution of the lobes refers to the dynamics of the moving particles, and after a long time this is different from what it is after a short time.

The organization of our paper is as follows. In Sec. II we give the main definitions that we use in this paper. In Sec. III we consider the forms of the lobes, their intersections, and their rotations around the resonance areas, for a particular value of the energy. In Sec. IV we explore how the structure of the lobes changes as the energy increases, and, in particular, when the energy exceeds the escape energy. In Sec. V we find the tangencies between lobes that lead to new stable and unstable periodic orbits, according to the Newhouse theorem, and finally Sec. VI contains our conclusions.

II. DEFINITIONS

We consider the main unstable periodic orbit in the 2D Hamiltonian system

$$H \equiv \tfrac{1}{2}(\dot{x}^2+\dot{y}^2+Ax^2+By^2)-\epsilon x^2 y = h \tag{1}$$

for $A=0.9$, $B=1.6$, $\epsilon=0.08$, and various values of the

energy h, and we study its asymptotic curves (stable and unstable manifolds on a Poincaré surface of a section). This periodic orbit is a resonant orbit of type $\frac{1}{2}$, i.e., it makes one oscillation along x and two oscillations along y during one period.

On the surface of section $x=0$ ($\dot{x}>0$) the Hamiltonian system is represented by a mapping and the main periodic orbit by a unique unstable (hyperbolic) invariant point O (Fig. 1). The mapping is defined by the first intersections $(y',\dot{y}')$ of orbits starting at points $(y,\dot{y})$ on the surface of section, by the same surface of section ($x=0$) and in the same direction ($\dot{x}>0$). The point $(y',\dot{y}')$ is called a (Poincaré) "consequent" of $(y,\dot{y})$.

The periodic orbit is unstable for $h>h_c\approx 22.17$. When $h>h_c$ there are two unstable asymptotic curves starting from O that we call U and UU (Fig. 1) in two opposite directions, and two stable asymptotic curves S and SS, also in two opposite directions. The asymptotic curves are the intersections of the unstable and stable manifolds

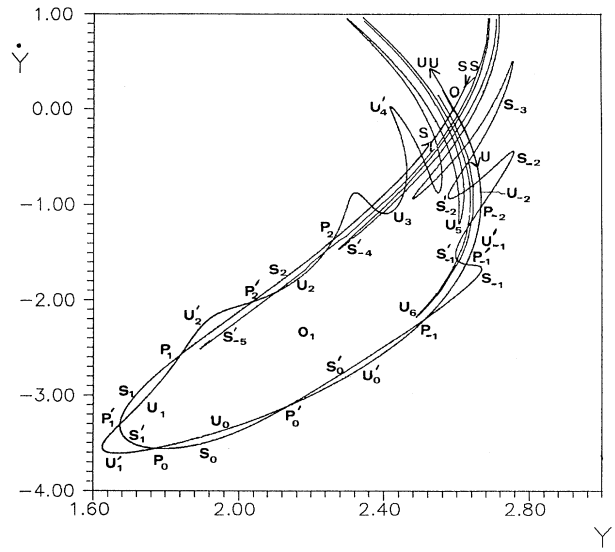

FIG. 1. Asymptotic curves from the unstable invariant point O on the surface of section $(y,\dot{y})$. We draw exactly (not schematically) the curves U (unstable) and S (stable), while we only indicate the directions of UU (unstable) and SS (stable) opposite to U and S. The initial homoclinic point P_0 is at roughly the same distance from O along the curves U and S and at this point the curve U crosses S outwards. The area contained between O and P_0 along the curves U and S is the resonance area O_1. An orbit starting at P_0 with $\dot{x}>0$ intersects the surface of section in the positive direction of time at the successive consequents (with $\dot{x}>0$), $P_1,P_2,\ldots$ and along the negative direction of time at $P_{-1},P_{-2},\ldots$. At the points P_n', between P_{n-1} and P_n, the orbit from P_0 intersects the surface of section with $\dot{x}<0$. The arcs $P_{n-1}P_n'$ along U and S are called U_n' and S_n' and define the lobe U_n' (outer) if $n\le 0$, or the lobe S_n' (inner) if $n\le 0$. The arcs $P_n'P_n$ along U and S are called U_n and S_n and define the lobe U_n (inner) if $n>0$ or S_n (outer) if $n\le 0$. The areas of successive lobes are equal. Because of the symmetry of the problem the curves UU and SS are symmetric to S and U, respectively. They define a resonance area O_2 and symmetric homoclinic points and lobes.

of the hyperbolic point O by the surface of section. The unstable hyperbolic point O is a regular one (not reflection hyperbolic), therefore points on the curves U, UU, S, and SS are mapped again on the same curves.

The numerical calculation of the lobes was made as follows. We started several hundreds or thousands of orbits with initial conditions along the eigenvectors U, UU in the positive time direction and along the eigenvectors S, SS in the negative time directions. In both cases we started very close to the unstable point O, and we calculated the successive Poincaré consequents (iterates of the mapping). The deviations of the initial points, on the eigenvectors, from the real asymptotic curves decrease by a factor λ (where λ is the largest eigenvalue of the point O) at every iteration. On the other hand, the deviations along the asymptotic curve increase by a factor λ, where λ is of order 2. Thus an initial error of order 10^{-16} (accuracy of double precision calculations) becomes large (of order 1) after about $n=16/\ln 2\approx 50$ iterations.

By comparing empirically orbits in double and quadruple precision we found that at least 80 successive double precision consequents are accurate to about the second decimal place. In cases where we had to go to longer periods we used quadruple precision, which is expected to give accurate positions up to $n\approx 160$ iterations. The calculated lobes refer to about $n=15$ iterations, and they are extremely accurate. Even the distribution of consequents up to about $n=140$, given in Fig. 8, in quadruple precision, is quite accurate. However, if we extend our calculations to much longer periods we find exponential deviations that affect not only the positions of individual consequents but also their overall distribution.

The curves U and S intersect each other at infinite homoclinic points. As an initial homoclinic point P_0 we consider one that is roughly at equal distances from O along U and S, *and* the U curve crosses the S curve at P_0 outwards. The area contained between the arcs OP_0 (along U) and the arc P_0O (along S) is called a resonance area. There are two resonance areas, O_1 and O_2, one below O and the other above it. If h is not very large ($h<26.78$), inside each resonance area we have a stable invariant point.

The consequents of P_0 in the forward time direction are $P_1,P_2,\ldots,P_n$ along the arc P_0O on the S curve, and they approach asymptotically O as $n\to\infty$ (Fig. 1). The consequents of P_0 in the backward time direction are $P_{-1},P_{-2},\ldots,P_{-n}$ and they also approach asymptotically O as $n\to\infty$. At every point P_n ($n>0$) the U curve crosses the arc P_0O outwards, while at every point P_{-n} the S curve crosses the arc OP_0 inwards in the positive time direction (into the resonance area). Between two successive points P_{n-1} and P_n, there is a point P_n' at which the curve U intersects the arc P_0O inwards, and between P_{-n-1} and P_{-n} there is a point P'_{-n} at which the curve S intersects the arc OP_0 outwards. We call U_n', S_n' the arcs of U and S between P_{n-1} and P_n' and U_n, S_n the arcs of U and S between P_n' and P_n (for $n\gtrless 0$).

The area between U_n' and S_n', or between U_n and S_n, is called a lobe. The lobes U_nS_n ($n>0$) are called U lobes ($U_1,U_2,\ldots$ in Fig. 1), and they start inwards towards the

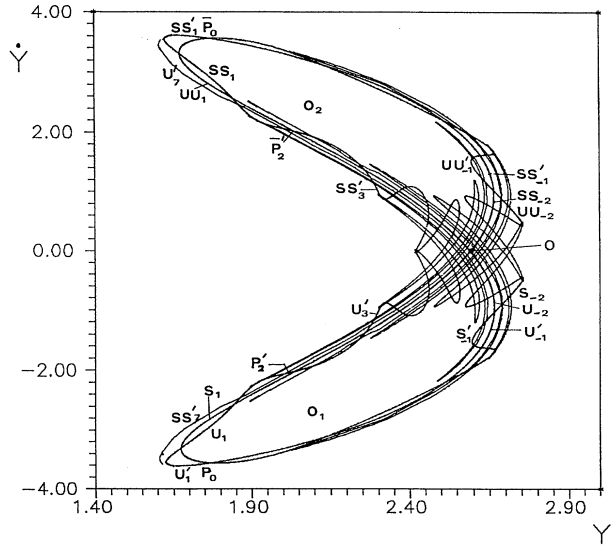

FIG. 2. The whole set of asymptotic curves U, S, and UU, SS. The points $\bar{P}_0, \bar{P}_1, \ldots$ are symmetric to $P_0, P_1, \ldots$, and the arcs UU_n, UU'_n, SS_n, SS'_n are symmetric to the arcs S_n, S'_n, U_n, U'_n, respectively. We notice that there are intersections not only between the lobes U and S', but also between the lobes U' and SS' and between the lobes UU' and SS, or between UU and S. (If we follow the asymptotic curves for longer times there are also intersections of the U' lobes with S, etc.)

resonance area O_1, while the lobes $U'_nS'_n$ are called U'_n lobes ($U'_1, U'_2, \ldots$), and they start outwards from the resonance area. For small n the whole lobes U_n are inside the resonance area, but for large n they may have a part outside it. Similarly for small n the whole lobes U'_n are outside the resonance area, but for large n they have a part inside it.

Similarly we have inner lobes S'_{-n} ($n \geq 0$) between U'_{-n} and S'_{-n} and outer lobes S_{-n} ($n \geq 0$) between U_{-n} and S_{-n}. These lobes are formed by the oscillations of the asymptotic curves S.

When n varies and takes both positive and negative values, we call a lobe U_nS_n either a U_n lobe or an S_n lobe, and a lobe $U'_nS'_n$ either a U'_n lobe or an S'_n lobe. In the same way we define the UU lobes and the SS lobes (Fig. 2).

III. THE STRUCTURE OF THE LOBES

It is obvious that the lobes U'_n ($=S'_n$) and U_n ($=S_n$) are mapped into U'_{n+1} ($=S'_{n+1}$) and U_{n+1} ($=S_{n+1}$) respectively, for all n. The corresponding areas are equal, because the system is Hamiltonian. Furthermore the areas between U'_n and S'_n and between U_n and S_n are equal because of the symmetry of the Hamiltonian with respect to x.

If two lobes intersect, so do their images. For example, in Fig. 1 ($h = 24$) the lobes S'_{-2} and U_5 intersect. Thus the lobes S'_{-3} and U_4 also intersect, and the common area is the same. The same is true for the lobes S'_{-4} and U_3, the lobes S'_{-5} and U_2 and so on. We can state this property as follows.

A U_m lobe intersects an infinity of S'_{-n} lobes up to a last S'_{-n} lobe with a minimum $n = n_0$. Then the previous U lobe (i.e., the lobe U_{m-1}) intersects all S'_{-n} lobes up to the previous S'_{-n} lobe (i.e., the last S'_{-n} lobe has then $n = n_0 + 1$).

This basic property is not seen in the intersections of the schematic lobes of the classical books of Moser [7] (see his Fig. 17), and Gutzwiller [8] (his Fig. 24). These figures represent the intersections of the U and S lobes but cannot be used to derive the details about the properties of these intersections. In order to find such details we need more accurate figures.

In order to see the form of the asymptotic curves for a longer interval we give in Fig. 3 the asymptotic curves U and UU up to a total of 100 orbits times 16 consequents each, equal to 1600 consequents, in Fig. 4 the asymptotic curve U up to a total of 2200 orbits times 15, equal to 33 000 consequents, and in Fig. 5 the asymptotic curve U up to 4000 orbits times 15, equal to 60 000 consequents.

In Fig. 2 we see that the UU_n, UU'_n and SS_n, SS'_n lobes are symmetric to the S_n, S'_n lobes and U_n, U'_n lobes, respectively, and the homoclinic points $\bar{P}_0, \bar{P}_1, \ldots$ are symmetric to $P_0, P_1, \ldots$. In Fig. 3 we give the lobes beyond the point $\bar{P}_0$ from UU_0 up to UU_{-5}, which are symmetric to the lobes S_0 to S_{-5} of Fig. 1, and the lobes UU'_{-1} to UU'_{-5}, symmetric to the lobes S'_{-1} to S'_{-5} of Fig. 1. We have also the outer lobes U'_1 to U'_7 and the inner lobes U_1 to U_6. In Fig. 4 we give the inner lobes up to U_{11} and the outer lobes up to U'_{12}.

In Fig. 1 we see that the inner U_m lobes with small m intersect only inner S'_{-n} lobes. However for larger m the inner U_m lobes also intersect SS'_n lobes (compare U_{11} of Fig. 4 and the SS'_n lobes of Fig. 2). On the other hand, the outer U'_m lobes intersect not only outer SS'_n lobes, but also outer S_{-n} lobes (compare the lobes U'_9, U'_{10} of Fig. 4 with the S_{-n} lobes of Fig. 2).

The outer lobes U'_n approach the curve UU close to O as n increases. However near the end points of the lobes U'_n the deviation from UU, which becomes smaller up to $n = 6$, increases for larger n.

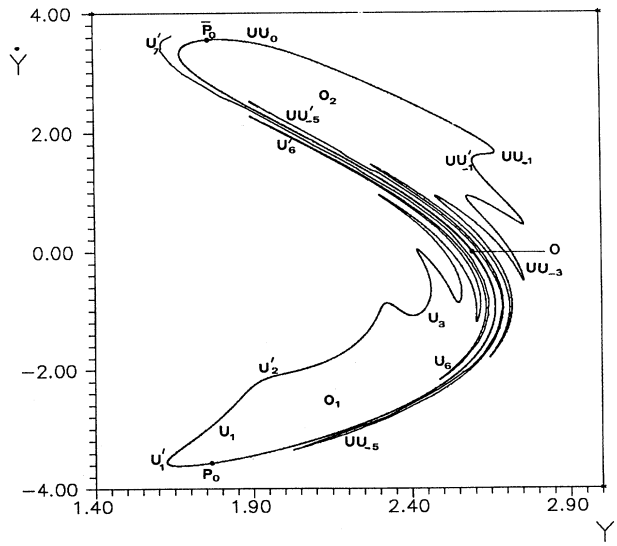

FIG. 3. The asymptotic curves U and UU up to the lobes U_6, U'_7 and UU_{-5}, UU'_{-5}.

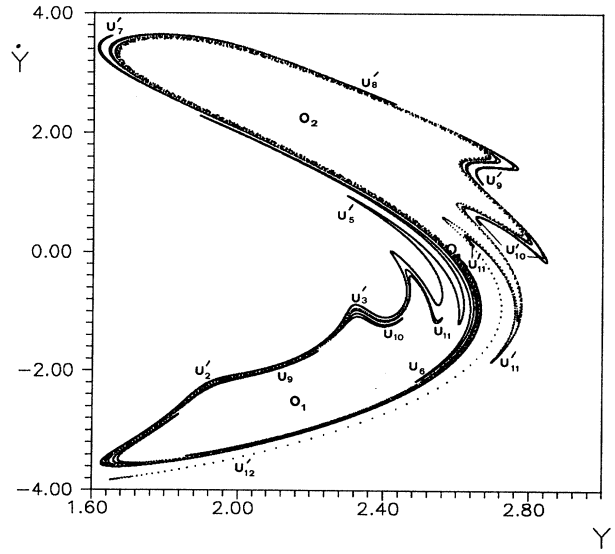

FIG. 4. The asymptotic curve U up to the lobes U_{11} and U'_{12}. We notice that the higher-order inner lobes U have parts that are outside the original resonance area O_1.

In Fig. 3 we see that the outer lobes U'_n tend to surround the resonance area O_2 in a clockwise direction. Similarly the UU_{-n} lobes tend to surround the resonance area O_1.

As the order n of the lobes U'_n increases beyond 7 the U'_n lobes surround more and more completely the resonance area O_2 (lobes $U'_8, U'_9, U'_{10}, U'_{11}$ of Fig. 4), and for even larger n the U'_n lobes tend to also surround the resonance area O_1 (U'_{12}). As n goes beyond 12, the tongues go around the resonance area O_1, then once more around the resonance area O_2, and so on.

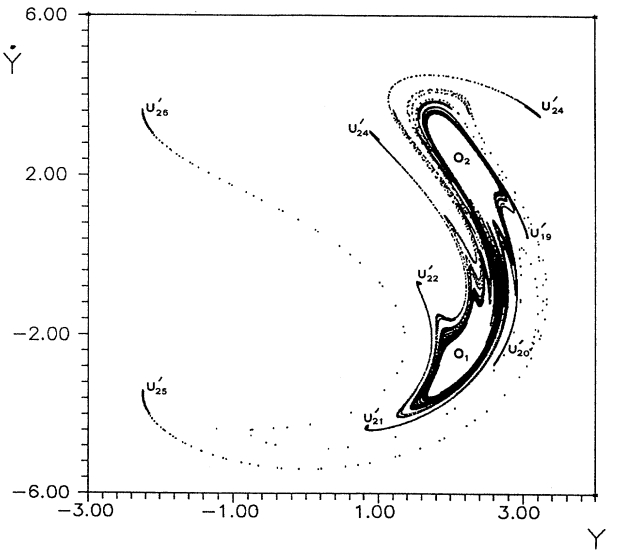

FIG. 5. The asymptotic curve U up to the lobe U'_{26}. The lobes up to U'_{18} are close to the resonance areas O_1O_2, while the higher-order lobes deviate further away. In particular the lobes U'_{25}, U'_{26} go quite far from O_1O_2.

In Fig. 4 we notice that while the end points of the lobes U'_5, U'_6, U'_7 are the most remote points from O along these lobes, in the case of the tongues U'_9, U'_{10}, U'_{11}, the end points are closer to O than the most remote points of the lobes. The most remote points $U'_1, \ldots, U'_{12}$ form a complete rotation around the point O, surrounding both resonant regions, O_1 and O_2.

The lengths of the higher-order lobes are of the order of λ^n, where λ is the largest eigenvalue of the unstable orbit O and n is the order of the lobes. This is due to the fact that the distance between P'_n and P_n decreases by a factor λ as n increases by one. Therefore as the areas of the lobes U_n and U_{n+1} are equal, the length of the lobe U_{n+1} is λ times larger than the length of the lobe U_n. We have checked numerically that this relation is satisfied close to the point O. However further away from O and close to P_0 the lengths of the lobes deviate from this simple relation. In Table I we give the lengths of several lobes and their ratios. We see that the ratios approach $\lambda=2.204$ or $1/\lambda=0.454$ as the order of the lobes increases.

It is difficult to draw the higher-order lobes because of the complexity of the figures. In Fig. 5 we give the lobes U'_n up to $n=26$. We notice that the lobes up to U'_{18} remain rather close to the resonant regions O_1, O_2, but later they extend to large distances from these resonant regions (compare the scales of Figs. 4 and 5).

The successive lobes pass between the previous lobes and the resonant regions, but extend further outwards. For example, the lobe U'_{10} in Fig. 4 is initially on the inner side of the lobe U'_9 (closer to the resonance area O_2), but then extends beyond U'_9 and further away from O_2. The lobe U'_{11} follows U'_{10}, but it goes beyond it and even further away from O_2. The same is true with the lobes U'_{12}, U'_{13}, U'_{14} that surround the resonance area O_1, and so on.

The lobe U'_{11} undergoes some oscillations near its end point, approaching and receding from the resonance area O_2. The lobes U'_{12}, U'_{13}, U'_{14} contain much longer oscillations along the left side of the area O_2 close to the curve

TABLE I. Lengths of lobes.

	Length	Ratio		Length	Ratio
U_1	0.734		S_1	0.742	
		1.07			1.08
U_2	0.686		S_2	0.684	
		1.32			1.86
U_3	0.521		S_3	0.367	
		0.53			2.02
U_4	0.977		S_4	0.182	
		0.46			2.14
U_5	2.106		S_5	0.085	
U'_2	0.612		S'_2	0.588	
		0.93			1.59
U'_3	0.655		S'_3	0.370	
		0.54			2.02
U'_4	1.205		S'_4	0.184	
		0.49			2.20
U'_5	2.472		S'_5	0.084	

UU. However we emphasize their outermost parts that surround in a clockwise direction the area O_1.

In Fig. 5 we see that the outermost lobes U'_{25}, U'_{26} reach distances from the resonance area O_1, O_2 that are larger than the total sizes of the resonance areas. Thus we may distinguish two regions occupied by the lobes. (1) The region around the resonances O_1, O_2, where the lobes are tightly wrapped, and (2) the region further away from O_1, O_2, where the lobes are more sparsely distributed. In the first case we have a localized chaotic behavior around O_1 and O_2, while in the second case the chaotic behavior is more extended.

In this larger region there are many resonance areas of different multiplicities, including several stable islands and asymptotic curves from various unstable periodic orbits. Our lobes avoid the stable islands and follow certain rules in their intersections with the asymptotic curves of other multiplicities. The intersections of the asymptotic curves of various types are planned to be discussed in a future paper. At any rate the appearance of heteroclinic intersections is the most prominent characteristic of chaos.

One way to get an idea of the structure of the higher-order lobes is by calculating a few orbits for a much longer time. Such a calculation is shown in Fig. 6. We mark 39 successive Poincaré consequents of an initial point B_0 ($y_0=2.612$, $\dot{y}_0=-0.8$, $x=0$, $\dot{x}>0$), located in the common area of the lobes U_5 and S'_{-2}. The consequent B_1 belongs to the common area of the lobes U_6 and S'_{-1}, and in general the consequent B_m belongs to the common area of the lobes U_{m+5} and S'_{m-2}.

We see that the consequents B_1 and B_2 are inside the resonance area O_1, but the consequents $B_3, B_4, B_5, \ldots$ are outside this area, although they belong to the "inner" lobes $U_7, U_8, U_9 \ldots$.

The consequents $B_1, \ldots, B_{15}$ make a complete rotation around the unstable point O, and B_{15} is close to B_0. Then the consequents continue in a clockwise spiral direction outwards, forming a second rotation up to B_{26}, a third rotation up to B_{36}, and a fourth rotation up to B_{46}. The consequents continue spiraling outwards up to B_{48} (Fig. 7). From then on they spiral inwards and then again outwards in a very irregular way, and cover the whole stochastic region. At this stage we have a large degree of chaos, covering a much larger area than the resonance areas O_1, O_2 (Fig. 7).

The total number of outward spiral rotations is 4, before most of the stochastic region is covered (sparsely) by the consequents B_n and the very irregular motion of these consequents sets in. The total number of outward spiral rotations decreases on the average as the energy increases.

The general arrangement of the consequents of B_0 is shown by the circles of Fig. 8. We see that the area covered by the scattered circles is a large part of the total available area, inside the circle defined by the energy integral. The stochastic region of Fig. 8 contains also other resonances and unstable periodic orbits of various multiplicities that form their own sets of asymptotic curves.

We have repeated the calculations of the consequents from two initial points B'_0 ($y_0=2.612$, $\dot{y}'_0=-0.73$) and B''_0 ($y_0=2.61$, $\dot{y}=-0.85$) very close to the point B_0, in the same common area of the lobes U_5 and S'_{-2}. The seven first consequents of B'_0 and B''_0 are quite close to B_1-B_7, but the subsequent consequents have greater deviations. The overall distribution of the points B'_m is similar to that of the points B_m. However the consequents B'_m move faster outwards. For example, the suc-

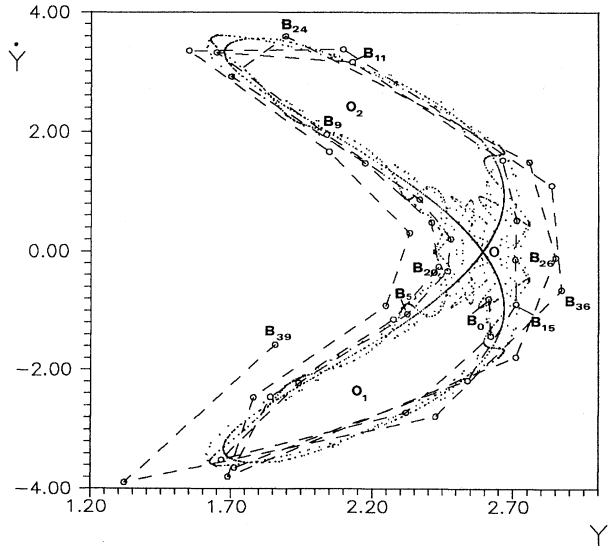

FIG. 6. The first 39 consequents of a point B_0 (located inside the intersection of the inner lobes U_5 and S'_{-2}). The successive consequents are joined by dashed lines. These lines spiral clockwise outwards.

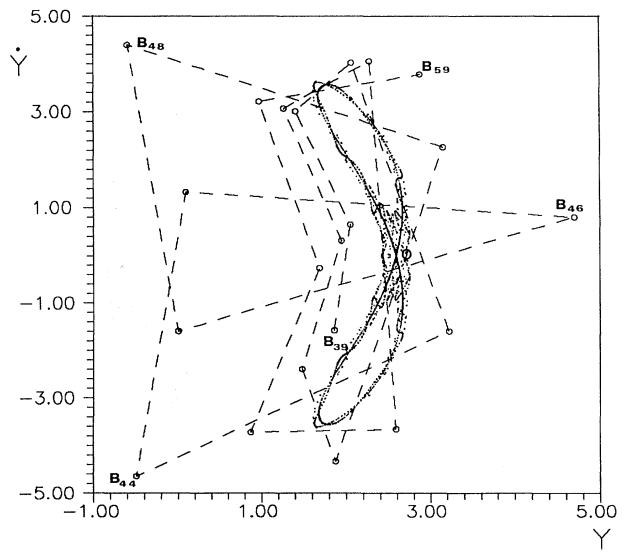

FIG. 7. Continuation of the consequents of B_0 from B_{39} to B_{59}. The lines joining successive consequents spiral clockwise outwards up to B_{48}, and from then on they move inwards and outwards in a very irregular way.

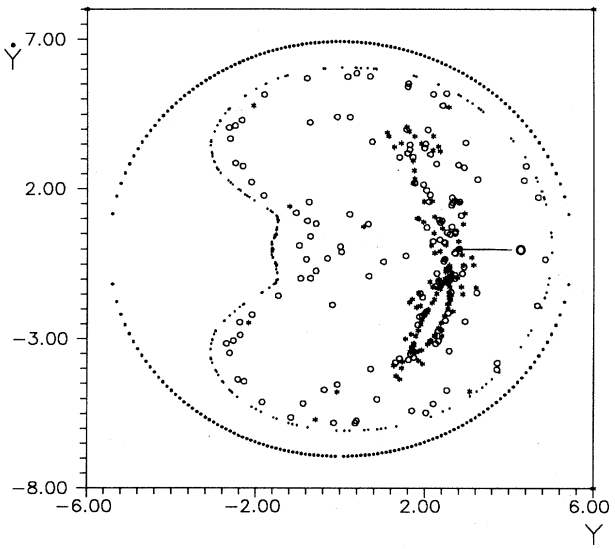

FIG. 8. The distribution of 140 successive consequents from B_0 (circles) and 140 successive consequents from A_0 (stars). The outer circle represents the boundary of the available space, defined by the energy integral, while the curve inside the boundary, defined by dots, represents one of the innermost well-defined KAM curves surrounding the stochastic region. Most of the area inside this curve is filled with chaotic orbits, but there are also some islands of stability, like those inside the resonance areas O_1 and O_2, defined in Fig. 1, where closed invariant curves also exist. Notice the difference of scales between Figs. 8, 7, and 6.

cessive clockwise rotations are completed at B'_{14}, B'_{23}, and before B'_{28}. After about three rotations around O_1, O_2, the consequents reach a maximum distance from the resonance areas and from then on they follow a very irregular pattern.

On the other hand, the consequents of B''_0 remain close to the resonance areas O_1, O_2 for extremely long times. Namely after one rotation around both O_1 and O_2 they make two rotations around O_2, one rotation around O_1, and then at least five rotations around both O_1 and O_2. We reached B''_{140} and the consequents are still close to the regions O_1, O_2.

We can "explain" the difference in behavior of the consequents of B_0, B'_0, B''_0 by following the elongated forms of the lobes to which they belong. For example, the consequents B_5, B'_5, B''_5 belong to the lobe U_{10}, which is inside the outer lobe U'_3 (Fig. 4). Similarly the consequents B_m, B'_m, B''_m belong to the lobe U_{m+5}, which is inside the lobe U'_{m-2}. However beyond $m=12$ the consequents B_m, B'_m move in a clockwise direction around O, surrounding both regions O_1, O_2, while B''_m remains for some time (up to B''_{27}) inside O_2. The corresponding lobes U_{m+5} are extremely elongated, and the distances of the points B_m, B'_m, B''_m become as large as the total dimensions of the resonance areas O_1, O_2. For example, for $m=24$ the point B_{24} is at the upper end of O_2, while B'_{24} is at the lower end of O_1. In a similar way for $m=18$ the point B''_{18} is at the upper end of O_2, while B_{18} is near the lower end of O_1. This implies that from then on there is practically no correlation between the behavior of B_m and B''_m or B'_m.

The deviation between nearby orbits increases exponentially in time. This is easily seen if we have points along an unstable asymptotic curve (U or UU) close to O. An initially small deviation D along this curve increases by a factor λ after one iteration, where λ is the maximum eigenvalue of O. Thus after m iterations the distance is of order $D\lambda^m$. A similar behavior appears for points outside the asymptotic curves. This exponential deviation leads to a positive maximal Lyapunov characteristic number.

We calculated also the consequents of a point A_0 ($y_0=2.612$, $\dot{y}_0=-01.0$, $x=0$, $\dot{x}>0$) which is near the end of the lobe U_5, below the lobe S'_{-3}. The consequents A_1-A_{40} make six rotations around the resonance area O_1, and then they spiral outwards around both resonance areas O_1 and O_2 up to A_{99}. From then on the consequents scatter in an irregular way over the whole stochastic region. In Fig. 9 we give the consequents $A_{69}-A_{99}$.

The deviations of the points A_m from the corresponding points B_m start to be important rather early. Namely, while both B_5 and A_5 belong to the lobe U_{10}, B_5 is inside the lobe U'_3, while A_5 is just outside the lobe U_3 (Fig. 4), which is a continuation of U'_3. The point A_7 is close to A_0, but outside the lobe U_5, while B_7 is well above A_7, in the lobe U'_5. From then on B_m ($m\geq 7$) moves upward and then rotates around O_2 and O_1, while the corresponding A_m makes several rotations inside O_1, before going out of O_1 beyond A_{40}. As a consequence the distribution of the consequents of A is rather different from that of the consequents of B for rather long times (Fig. 8).

The consequents of A_0 are given as stars in Fig. 8 for

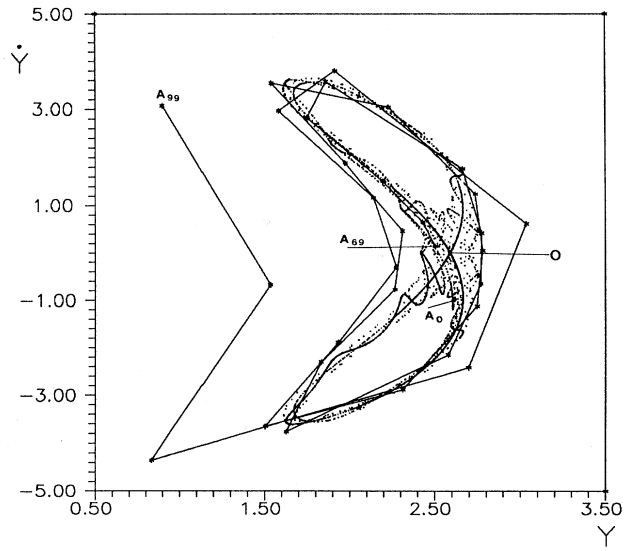

FIG. 9. Some of the successive consequents of A_0 (near the end of the inner lobe U_5). The consequents up to A_{39} are trapped inside the resonance region O_1, while the consequents from $A_{39}-A_{99}$ are outside the resonance regions O_1 and O_2. The successive consequents from $A_{69}-A_{99}$ are joined by straight lines, and they spiral clockwise outwards.

about the same time interval as the consequents of B_0 (circles). This figure contains 140 circles and 140 stars, calculated in quadruple precision, and their positions are more accurate than the sizes of the stars and circles. The overall distribution of the stars seems much more concentrated close to the outer boundaries of the resonant regions O_1 and O_2 than the distribution of the circles. However the stars actually extend as far away from O as the circles, and we do see some stars far away from O. But the density of the stars is quite different from that of the circles for very long times (up to $m > 140$). Therefore the chaotic behavior of the consequents of two points (B_0 and A_0) that are initially rather close along the same U lobe is rather different, although it is expected that after even longer times their average distribution should be similar. Similar results were found for the consequents of points initially close to A_0.

The rotation of the outer lobes U'_n, S_{-n}, and UU_{-n}, SS'_n around the resonance areas O_1, O_2 explain the "stickiness property" of the outermost KAM curves surrounding stable invariant points. In the present case the invariant points O_1, O_2 are surrounded by closed invariant curves that extend outwards up to the inner limit of the homoclinic tangle produced by the asymptotic curves of O. The outermost KAM curves are not well defined. The outer KAM curves around O_1, or O_2, form more and more corrugations as they approach the higher-order inner lobes of the homoclinic tangle, and the outermost KAM curve should be a fractal [9,10]. The case that we consider here is different from the "destruction" of the "last KAM curve" with a golden rotation number [11], when the perturbation parameter μ of a system goes beyond a critical value, μ_c. The last KAM curve for $\mu=\mu_c$ is a fractal, and it becomes a cantorus for larger μ. In the present case, however, we consider the outermost KAM curve among the invariant curves of the island O_1, for a fixed value of the energy, which is also a fractal. This case is also quite general.

If we start an orbit within a lobe in one of the resonance areas O_1, O_2, this orbit follows the images of this lobe and makes several rotations around the resonance areas O_1, O_2 before going far away. Thus, although the stochastic region is much larger than both resonance areas O_1, O_2, the successive consequents stay close to the resonance areas for a long time (of the order of $n=30-150$) before going away from these resonance areas (Figs. 6–8).

This is why the resonance areas are sticky, i.e., the consequents of initial points in their neighborhood stay close to them for a long time before going far away. This time is larger for smaller energies h and decreases as h increases. The stickiness phenomenon was observed in numerical experiments by Contopoulos [12] in a problem equivalent to the present Hamiltonian (1). The term "stickiness" was introduced by Shirts and Reinhardt [13], and this property has been emphasized by various authors [14].

As we have seen, the deeper reason for the stickiness phenomenon is connected with the form of the lobes in the homoclinic tangle of an unstable periodic orbit. We may say that as long as the lobes rotate close to the resonance areas we have partial order, and chaos is not complete. Only when the lobes occupy the whole stochastic region we have well-established chaos, and no more a sticky behavior.

IV. THE LOBES FOR LARGER ENERGIES

When the energy increases from $h=24$ to $h=24.5$ and $h=25$ the forms of the asymptotic curves are qualitatively similar, but they have several quantitative differences.

Figure 10 gives the asymptotic curves U and S that form a few lobes U, U', S, S' in the case $h=24.5$. If we compare this figure with Fig. 1 we see the following changes.

(i) The resonance area O_1 is larger.

(ii) The lengths and the areas of the lobes are much larger.

(iii) There are new intersections of the lobes U and S'. For example, in Fig. 1 the lobes S'_{-3} intersects the lobes U_4, U_5, etc. But in Fig. 10 the lobe S'_{-3} intersects also the lobes U_3 and U_2.

The case $h=25$ is even more extreme, as shown in Figs. 11 and 12, in comparison with Figs. 1 and 4. The lobe U'_4 already surrounds the resonance area O_2, roughly to the extent of the lobe U'_8 of the case $h=24$. The lobe U'_5 makes almost $1\frac{1}{2}$ rotations around O and reaches a large distance from O, deviating considerably from the resonance area O_1. The lobe U'_6 also deviates considerably from the resonance areas. This extends roughly to the distance of the lobe U'_{26} of $h=24$. The lobes U'_5, U'_6, U'_7 reach almost the maximum possible distance from O inside the outer last KAM curve that surrounds the whole stochastic region around O.

In Fig. 13 we give the area of a lobe as a function of the eigenvalue λ of the periodic orbit O. For $\lambda=1$ the area A is zero. For small values of $(\lambda-1)$ the area A increases roughly as $(\lambda-1)^{6.5}$, but for $\lambda \gtrsim 2.7$ (i.e., $h \gtrsim 25$) A increases roughly as $(\lambda-1)^4$. As a consequence the lengths

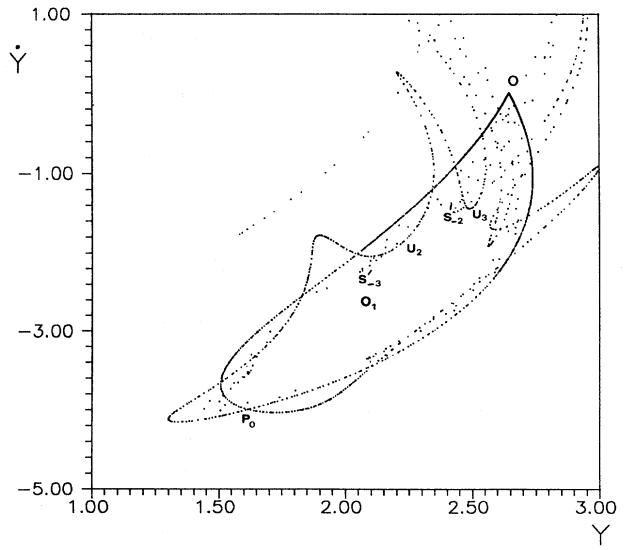

FIG. 10. The asymptotic curves U and S in the case $h=24.5$. Compare with Fig. 1, noticing the difference of scales.

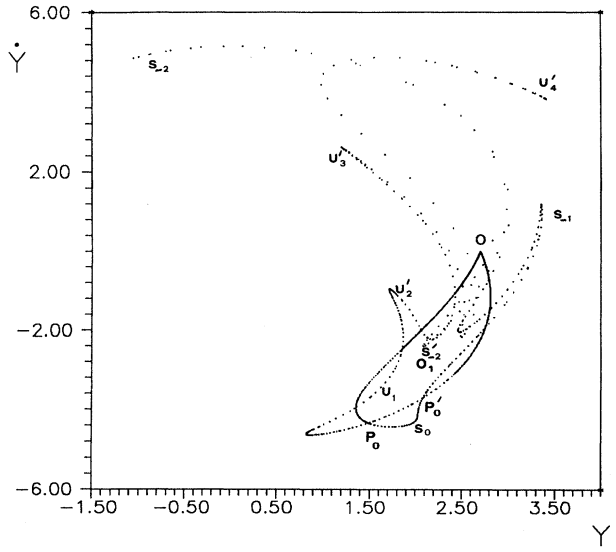

FIG. 11. The asymptotic curves U and S in the case $h=25$ up to the lobes U'_4 and S_{-2}. Compare with Fig. 1, noticing the difference of scales.

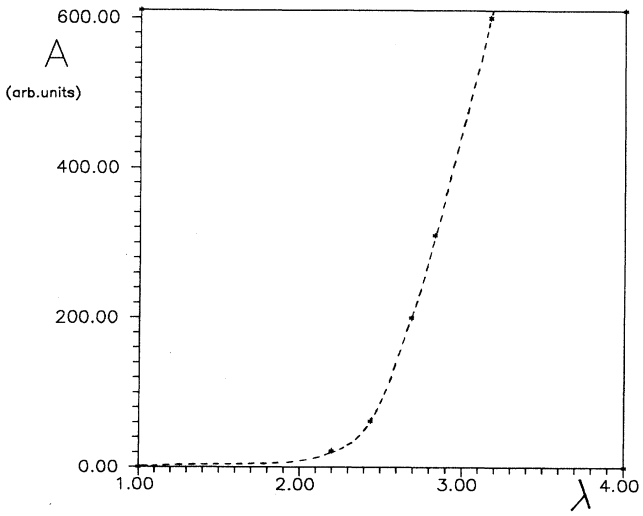

FIG. 13. The area of a lobe (in arbitrary units) as a function of the maximum eigenvalue λ of the periodic orbit O.

of the lobes of the same order n increase considerably with the energy. As h increases even further we have two more new phenomena.

(iv) The lobe U'_1 becomes so elongated and deformed that it crosses the line S between P'_1 and P_1 and enters the resonance area O_1 (Fig. 14, $h=27.80$). At the same time the lobes U_1 and S'_0 are almost tangent inside the resonance area O_1. Thus there is no stable region inside the resonance area. In fact the orbit O_1 becomes unstable for $h=26.78$. For still larger h the lobe U'_1 itself invades a large part of the resonance area O_1.

(v) If h becomes larger than the escape energy $h_{esc}=25.31$, some asymptotic orbits go to infinity. In the present problem the equipotentials for $h>h_{esc}$ have two openings that we call escape channels, because orbits passing through any such opening extend in general to infinity. At every such opening there is an unstable periodic orbit, usually called a Lyapunov orbit, which is close to a straight line bridging the opening. Every orbit crossing such a Lyapunov orbit outwards escapes to infinity [15,6].

The asymptotic curves of any given unstable periodic orbit that intersect the asymptotic curves of a particular Lyapunov orbit make infinite spiral rotations, around a

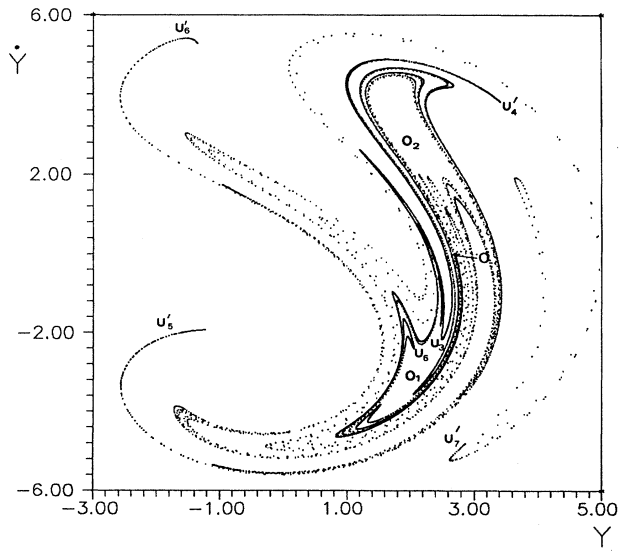

FIG. 12. The asymptotic curve U in the case $h=25$ up to U'_7 and U_6. Compare with Fig. 4. Notice the very great difference of scales.

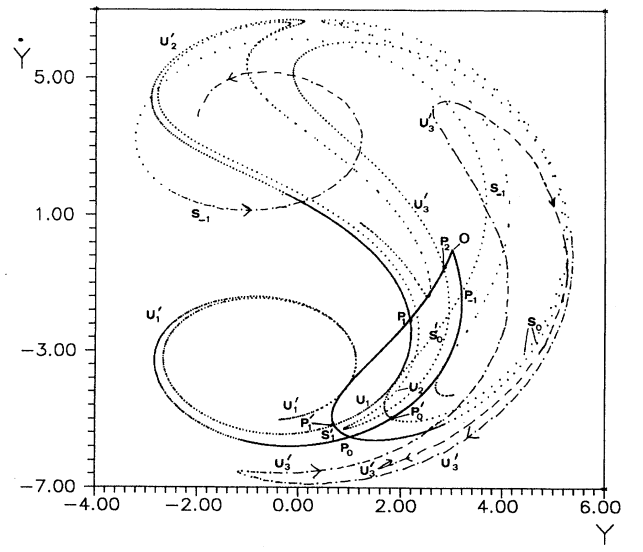

FIG. 14. The asymptotic curves U and S in the case $h=27.80$. The lobe U'_1 is very elongated and intersects the line S between P'_1 and P_1 (there are two intersection points as we proceed from P_0 towards the end point of the lobe, and two more when we return towards P'_1). The curves S'_0 and U_1 are almost tangent.

special curve, called a "limiting asymptotic curve" [6]. This curve is the intersection of the surface of section by the 3D asymptotic surface (unstable manifold) of the Lyapunov orbit. Such a spiral is the curve U_3' for $h=27.8$ (Fig. 14), which forms infinite clockwise rotations and tends to a limiting asymptotic curve on the right of the point O.

In the case of the Hamiltonian (1) there are two escape channels, and each channel is crossed by a Lyapunov orbit (Fig. 10 of Contopoulos [6]). In the present case the axes (x,y) are interchanged with respect to our previous paper [6], and the escape channels are upwards and to the right or the left. The asymptotic orbits may escape (when $t\to+\infty$) either upwards and to the left (going to $x=-\infty$, $y=\infty$), or upwards and to the right (going to $x=\infty$, $y=\infty$). The curve U_1' for $h=31.3$ (Fig. 15) tends to the first limiting asymptotic curve, and the orbits escape to the right, while the curve U_3' for $h=27.8$ (Fig. 14) tends to the second limiting asymptotic curve, and the orbits escape to the left.

The limiting asymptotic curves are formed immediately as h increases beyond the escape energy $h=25.31$. However a particular lobe is transformed into a spiral with infinite rotations about a particular limiting asymptotic curve only after h goes beyond a critical value h_c'. This critical value depends on the particular lobe considered. For example, the lobe U_3' tends to a spiral for $h=h_c'$ smaller than the critical value $h=h_c$ required for U_1' to form another spiral.

In the same way we have two limiting asymptotic curves as $t\to-\infty$. These are symmetric to the limiting asymptotic curves for $t\to+\infty$ with respect to the axis $\dot{y}=0$, and they are limits of S_{-n} lobes. For example, the curve S_{-1} in Fig. 14 forms infinite rotations and spirals inwards, in a counterclockwise direction, to a limiting asymptotic curve for $t\to-\infty$. The orbits starting along the curve S_{-1} escape to the left ($x=-\infty$, $y=\infty$) as $t\to-\infty$. This limiting asymptotic curve is symmetric to the limiting asymptotic curve for $t\to+\infty$ reached by the curve U_1' in Fig. 15. This symmetry is due to the symmetry of the Hamiltonian (1) with respect to x (but of course the size of the limiting asymptotic curves changes with the energy h). In Fig. 14 ($h=27.8$) the lobe U_1' has not yet reached the form of infinite spirals. It reaches this form for h between $h=27.8$ and $h=31.3$.

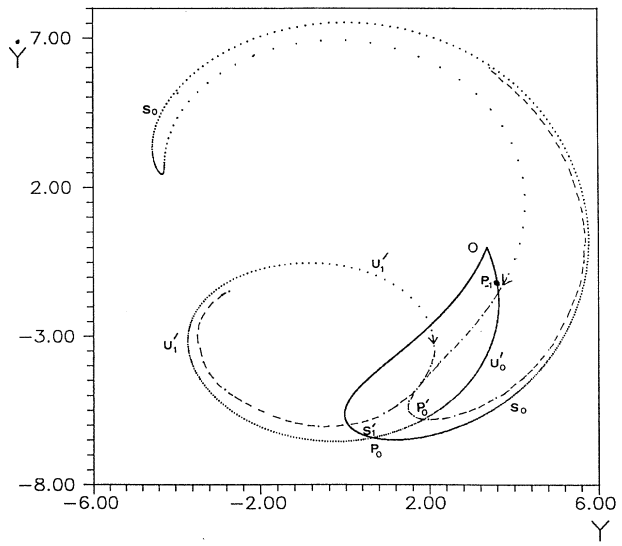

FIG. 15. The asymptotic curves U and S in the case $h=31.30$. The asymptotic curve U_1' (beyond P_0) forms infinite clockwise spiral rotations inwards, tending to a limiting asymptotic curve. The curve U_1' is almost tangent to the inner lobe S_0'.

In a similar way the curve S_0 in Fig. 15 ($h=31.3$) spirals, in a counterclockwise direction, towards a limiting asymptotic curve as $t\to-\infty$, which is symmetric to the limiting asymptotic curve for $t\to+\infty$, that is reached by the curve U_3' for $h=27.8$ (Fig. 14). The orbits starting along S_0 escape to the right ($x=\infty$, $y=\infty$ as $t\to-\infty$). By comparing Figs. 14 and 15 we see that the limiting asymptotic curves reached by U_3' and S_0 intersect, while the limiting asymptotic curves reached by S_{-1} and U_1' are well separated.

The asymptotic curve U_1' of Fig. 15 has infinite length and does not return to form a complete lobe. Thus we do not have any consequents $P_1', P_1, \ldots$. This means that the orbit starting at P_0 upwards (with $\dot{x}>0$) escapes to infinity and does not intersect again the surface of section $x=0$ downwards (with $\dot{x}<0$). The same is true for orbits starting along the arc OP_0 of U, a little before P_0. However orbits starting close to O do intersect the surface of section again. The orbit starting at P_{-1} (Fig. 15) intersects the U curve downwards (with $\dot{x}<0$) at P_0' and upwards (with $\dot{x}>0$) at P_0. If we start orbits with $\dot{x}>0$ and initial conditions along $P_{-1}P_0'$, beginning at P_{-1}, we have the next consequents with $\dot{x}>0$ along U_1', beyond P_0. But as we proceed towards P_0' the consequents of the orbits with initial $\dot{x}>0$ disappear, before the initial point reaches P_0', because the orbits extend to infinity. There is a limiting point between P_{-1} and P_0' that separates the orbits that escape from those that do not escape before the next consequent with $\dot{x}>0$. This point is a heteroclinic point representing a doubly asymptotic orbit that approaches a Lyapunov orbit as $t\to+\infty$ and the resonant $\frac{1}{2}$ orbit as $t\to-\infty$. This phenomenon was described by Contopoulos [6].

As we proceed beyond this heteroclinic point along the curve $P_{-1}P_0$ we find further heteroclinic points and arcs of the asymptotic curve, starting and ending at the same limiting asymptotic curve. This phenomenon we found earlier [6] for the asymptotic curve of a Lyapunov orbit, but we verified that it is also valid for the asymptotic curve of the $\frac{1}{2}$ orbit, which we study here.

V. TANGENCIES

A comparison of Figs. 1 and 10 shows that as h increases the various lobes increase their number of intersections. Thus it is of interest to see how these new intersections are produced.

For $h=24$ the lobe S'_{-2} intersects the lobe U_5 but not U_4. Similarly the lobe S'_{-3} intersects U_4 but not U_3.

When $h=24.065$ all the lobes become longer, and the

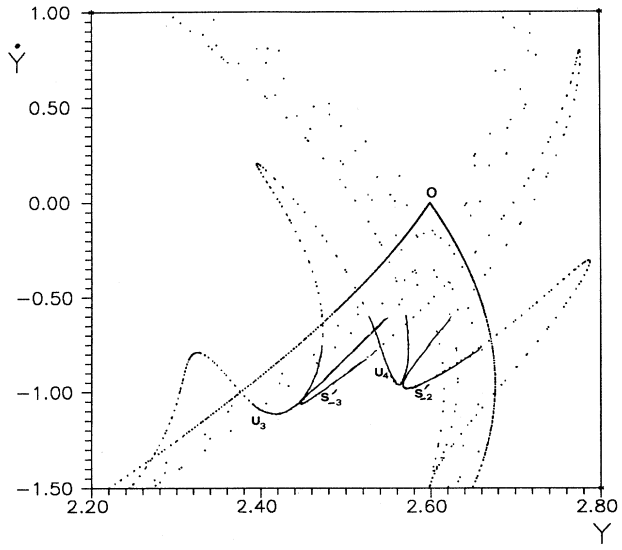

FIG. 16. The tangency of the lobes U_4, S'_{-2} and of U_3, S'_{-3}, etc. for $h=24.05$.

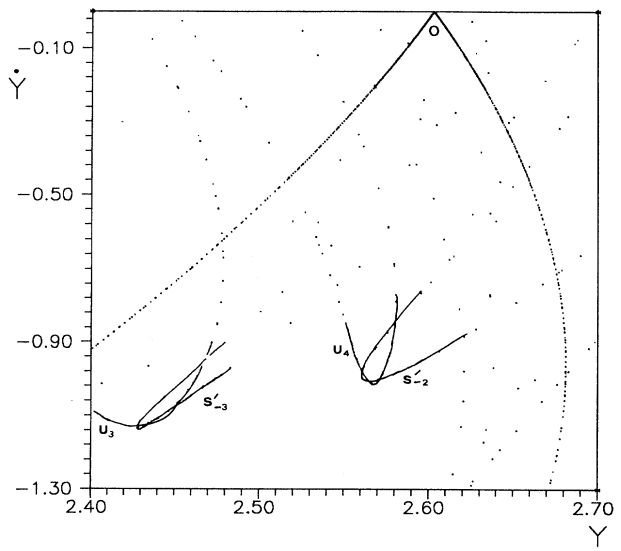

FIG. 18. The lobes S'_{-2} and S'_{-3} pass through the lobes U_4, U_3, respectively, for $h=24.1$.

lobes S'_{-2} and U_4 are tangent (Fig. 16). Also the lobes S'_{-3} and U_3 are tangent. In general the lobes U_m and S'_{m-6} are tangent.

When $h=24.075$ the lobes S'_{-2}, U_4 and S'_{-3}, U_{-1} intersect (Fig. 17). When $h=24.1$ the lobes S'_{-2}, U_4 pass through each other and the same happens with the lobes S'_{-3}, U_3 (Fig. 18).

In the transition case between Figs. 17 and 18 it seems that the curves S'_{-2} and U_4 have an odd tangency, i.e., they are tangent and at the same time they cross each other. This happens for $h\approx 24.095$.

As h increases further the lobes become longer and even further tangencies appear. As we remarked already, for $h=24.5$ the lobe S'_{-3} crosses not only the lobe U_4 but

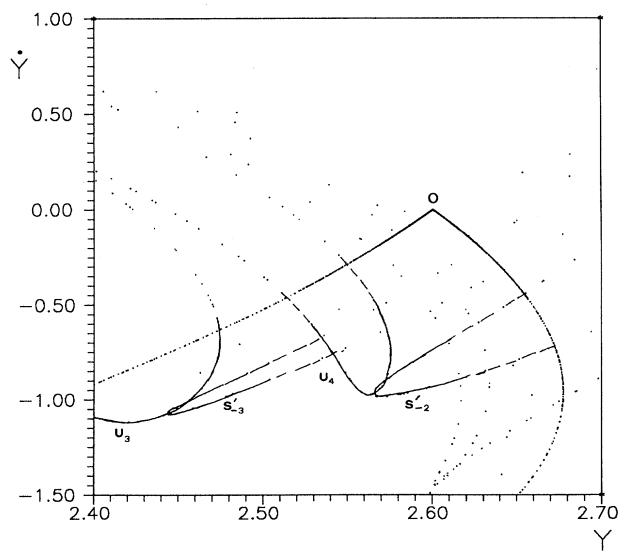

FIG. 17. The lobes U_4,S'_{-2} and U_3,S'_{-3} intersect for $h=24.075$.

also the lobes U_3 and U_2. Similarly the lobe S'_{-2} crosses not only the lobe U_5, but also the lobes U_4 and U_3. When $h=25$ the lobe S'_{-2} intersects not only the lobe U_3, but also the lobe U_2.

This increase in the number of intersections of the lobes is a natural consequence of the lengthening of the lobes, which in turn is due to the increase of the eigenvalue λ of the periodic orbit O as the energy increases.

The increase in the number of intersections of the lobes increases the degree of stochasticity and diffusion in phase space, because it produces faster mixing of the various regions of phase space. A particular case of a tangency of the lobes S'_{-2} with U_1, S'_{-3} with U_0, etc. followed by a corresponding large degree of chaos is shown in Fig. 19.

Another consequence of the new tangencies is the following. Whenever two lobes are tangent the theorem of Newhouse [16,17] shows the existence of nearby stable periodic orbits. These orbits disappear when h is reduced and the tangency disappears. Therefore these orbits are not generated by bifurcation of other periodic orbits, but they are "irregular" orbits [18], generated by a tangent bifurcation in a pair of a stable and an unstable periodic orbit. All these stable periodic orbits become unstable after an infinite cascade of periodic doubling bifurcations for a little larger h. However for an interval Δh of values of h there are stable periodic orbits, surrounded by corresponding islands of stability.

As h increases there appear more and more new tangencies of the various lobes that produce new stable periodic orbits and new islands of stability. We conjecture that in a bounded system for arbitrarily large energies h (or perturbations) there are intervals (Δh) for which chaos is not complete, but the phase space contains islands of stability. In other words there is no value of h beyond which chaos is complete.

However if the phase space is unbounded (for h larger

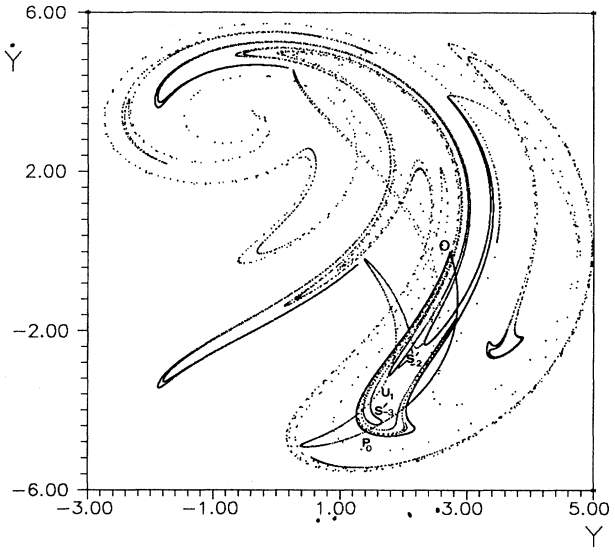

FIG. 19. The intersections of the asymptotic curves U and S in the case $h=25.3242$ when we have tangencies $S_{-2}U_1$, $S_{-3}U_0$, etc.

than the escape energy h_{esc}) the number of tangencies of the main lobes, as h increases, is finite. In the present model we give the tangencies for the corresponding values of h and λ in Table II. We give also the differences $\Delta h, \Delta\lambda$ and the ratios δ and δ' of the successive Δh and $\Delta\lambda$, and we notice that these ratios are almost equal.

The last case of Table II is close to that of Fig. 14. If h increases to $h=31.30$ (Fig. 15) the lobe U_1' enters into the resonance area O_1 and becomes tangent to S_0'. However in this case we cannot find more tangencies (like $U_2'S_1'$), because the lobe U_1' terminates, after infinite spiral rotations, at a limiting asymptotic curve, and there are no branches U_2', U_3', etc. This means that the sequence of tangencies terminates because the asymptotic curves terminate due to escapes.

As h decreases, we have infinite higher-order tangencies that tend to the value $h=h_0=22.17$ at which the periodic orbit O becomes stable. Therefore the intervals Δh become smaller and smaller, as $h\to h_0$, and the ratios δ tend to 1.

On the other hand, as h increases beyond $h=h_{esc}=25.31$, some lobes become incomplete because of escapes, and the sequence of tangencies terminates.

VI. CONCLUSIONS

We have studied the asymptotic curves from an unstable invariant point O, representing a periodic orbit of order $\frac{1}{2}$, in the Hamiltonian $H\equiv\frac{1}{2}(\dot{x}^2+\dot{y}^2+Ax^2+By^2)-\epsilon x^2y=h$, for various values of the energy h. The asymptotic curves are the intersections of the unstable and stable manifolds of the periodic orbit by a Poincaré surface of section. The unstable asymptotic curves U, UU intersect the stable asymptotic curves S, SS at infinite homoclinic points and form infinite lobes, on the surface of section, that create the so-called homoclinic tangle. We studied the behavior of these lobes as their order increases.

In the present model there is a symmetry between the curves U, S and SS, UU, respectively. The curves U and S from O up to the main homoclinic point P_0 opposite to O, define a resonance area O_1 and the curves UU, SS a symmetric resonance area O_2.

Some conclusions of the present study are the following.

(1) The intersections of the lobes U and S' follow certain rules. For example, if U_m and S'_{-n} intersect, so do U_{m+k} and S'_{-n+k}, for any integer k, positive or negative.

(2) The outer lobes U_n' tend to rotate in a clockwise way around the resonance area O_2. As n increases, they spiral outwards, surrounding both resonance areas, O_1 and O_2. The inner lobes U_n go also outside the resonance area O_1, surrounding O_1 and O_2.

The lobes UU_n', UU_n form similar spirals. The spirals U_n', U_n and UU_n', UU_n surround one another.

(3) The lobes remain close to the resonance areas O_1, O_2, up to a certain order n. This behavior explains the "stickiness" property of the resonance areas.

(4) As the order n increases beyond a certain number,

TABLE II. The energies and eigenvalues at various tangencies.

Tangencies	h	Δh	δ	λ	$\Delta\lambda$	δ'
$U_mS'_{m-7}(\ldots U_4S'_{-3},U_3S'_{-4},\ldots)$	23.859			2.1355		
		0.206			0.1000	
$U_mS'_{m-6}(\ldots U_4S'_{-2},U_3S'_{-3},\ldots)$	24.065		0.74	2.2355		0.74
		0.280			0.1349	
$U_mS'_{m-5}(\ldots U_3S'_{-2},U_2S'_{-3},\ldots)$	24.345		0.70	2.3704		0.70
		0.400			0.1921	
$U_mS'_{m-4}(\ldots U_3S'_{-1},U_2S'_{-2},\ldots)$	24.745		0.67	2.5625		0.67
		0.597			0.2882	
$U_mS'_{m-3}(\ldots U_2,S'_{-1},U_1S'_{-2},\ldots)$	25.342		0.63	2.8507		0.62
		0.948			0.4679	
$U_mS'_{m-2}(\ldots U_2S'_0,U_1S'_{-1},\ldots)$	26.290		0.61	3.3186		0.58
		1.550			0.8056	
$U_mS'_{m-1}(\ldots U_2S'_1,U_1S'_0,\ldots)$	27.840			4.1242		

the spiral lobes deviate away from the resonance areas O_1, O_2. They reach a maximum distance from O and from then on the lobes are very irregular, covering the whole available space inside the outer KAM curves (that surround the whole stochastic region around O).

(5) The number of spiral rotations of the consequents, close to the resonance areas O_1, O_2, depends on the initial conditions. Slightly different initial conditions give different numbers of spiral rotations. However the average number of rotations decreases as the energy h increases.

(6) The length of each successive lobe is roughly λ times longer than the previous one, where λ is the largest eigenvalue of O. Thus the length of a lobe of order n is of the order of λ^n.

(7) As h increases the resonance areas increase, and the areas of the lobes increase considerably (as a high power of the eigenvalue λ).

(8) The number of intersections of the various lobes increases as h increases. For example, for $h=24$ the lobe S'_{-2} intersects U_5, U_6, and all higher-order U lobes; for $h=24.5$ the lobe S'_{-2} intersects also U_4 and U_3, and for $h=25$ it intersects also the lobe U_2. The larger number of intersections produces a larger degree of mixing of the phase space, therefore chaos appears faster.

(9) As the lobes S' become longer with h they become tangent to new lobes U for certain values of h. Then new stable periodic orbits are formed nearby, which exist for a small range Δh of values of h before they become unstable, by period doubling cascades.

(10) New tangencies, and therefore new stable periodic orbits, appear for arbitrarily large h in a bounded system. On the other hand, in an unbounded system the number of tangencies reaches a maximum as h increases, but from then on the asymptotic curves terminate because of escapes.

(11) When the energy h increases beyond the escape energy $h_{\rm esc}$, some orbits escape to infinity. In the present case the equipotentials for $h > h_{\rm esc}$ have two openings that are crossed by two unstable periodic orbits, called Lyapunov orbits. Any orbit crossing a Lyapunov orbit outwards escapes from the system. Such an orbit, starting at a given initial point P in the positive (negative) time direction, has a finite number of intersections with the Poincaré surface of section as $t \to +\infty$ ($t \to -\infty$).

(12) When $h > h_{\rm esc}$ the asymptotic curves of some unstable periodic orbits terminate at particular limiting asymptotic curves. In the present model there are four limiting asymptotic curves, formed by the asymptotic curves of the two Lyapunov orbits. Two of them correspond to orbits escaping as $t \to +\infty$ and two more correspond to orbits escaping as $t \to -\infty$. The characteristic curves of unstable periodic orbits leading to escapes terminate by making infinite spiral rotations around these limiting asymptotic curves.

[1] H. Poincaré, *Méthodes Nouvelles de la Mécanique Céleste,* (Gauthier Villars, Paris, 1899), Vol. III.

[2] J. Guckenheimer and P. Holmes, *Nonlinear Oscillations, Dynamical Systems, and Bifurcations of Vector Fields* (Springer-Verlag, New York, 1983).

[3] S. Wiggins, *Global Bifurcations and Chaos: Analytical Methods* (Springer-Verlag, New York, 1988).

[4] S. Wiggins, *Introduction to Applied Nonlinear Dynamical Systems and Chaos* (Springer-Verlag, New York, 1990).

[5] V. Rom-Kedar and S. Wiggins, Arch. Rat. Mech. Anal. **109**, 231 (1990).

[6] G. Contopoulos, Astron. Astrophys. **231**, 41 (1990).

[7] J. Moser, *Stable and Random Motions in Dynamical Systems* (Princeton University Press, Princeton, NJ, 1973).

[8] M. C. Gutzwiller, *Chaos in Classical and Quantum Mechanics* (Springer-Verlag, New York, 1990).

[9] G. Schmidt and J. Bialek, Physica D **5**, 397 (1982).

[10] A. J. Lichtenberg and M. A. Lieberman, *Regular and Stochastic Motion* (Springer-Verlag, New York, 1983).

[11] S. J. Shenker and L. P. Kadanoff, J. Stat. Phys. **27**, 631 (1982).

[12] G. Contopoulos, Astron. J. **76**, 147 (1971).

[13] R. B. Shirts and W. P. Reinhardt, J. Chem. Phys. **77**, 5204 (1982).

[14] C. R. Menyuk, Phys. Rev. A **31**, 3282 (1985), and references therein.

[15] R. C. Churchill, G. Pecelli, and D. L. Rod, in *Stochastic Behavior in Classical and Quantum Hamiltonian Systems,* edited by G. Casati and J. Ford (Springer-Verlag, Heidelberg, 1979), p. 76.

[16] S. E. Newhouse, Am. J. Math. **90**, 1061 (1977).

[17] S. E. Newhouse, *Chaotic Behavior of Deterministic Systems,* edited by G. Iooss, R. H. G. Helleman, and R. Stora (North-Holland, Amsterdam, 1983), p. 443.

[18] G. Contopoulos, Astron. J. **75**, 96 (1970).